Mon. Not. R. Astron. Soc. (1992) **259**, 175–190

X-ray spectra of eight Seyfert galaxies

K. K. Ghosh and S. Soundararajaperumal
Indian Institute of Astrophysics, Vainu Bappu Observatory, Kavalur, Alangayam, NA, TN, 635701 India

Accepted 1992 May 7. Received 1992 May 7; in original form 1991 August 18

ABSTRACT

Analyses of the low- (LE) and medium-energy (ME) X-ray (0.1–10 keV) spectra of eight Seyfert galaxies (ESO 012–G21, Mkn 352, Mkn 374, Mkn 766, Mkn 279, Mkn 464, Mkn 290 and ESO 140–G43), obtained from the *EXOSAT* data base, are presented. For seven of these galaxies, power-law plus absorption models fit the LE plus ME spectra well, although the low-energy absorption (N_H) values are smaller than the corresponding galactic N_H values. For ESO 140–G43, a power-law plus fixed-absorption model is unacceptable, because of the large values of the reduced χ^2 ($\chi^2_r \gg 1.0$). Seven of the galaxies (ESO 012–G21, Mkn 352, 374, 766, 279, 464 and 290) have soft excesses in their spectra when they are fitted with the fixed power-law (obtained from the fits to the ME data) plus fixed-absorption model. For six of them, this is a new result. Models involving two power laws, thermal bremsstrahlung and broken power laws were tried in attempts to fit the soft excesses, but they were fitted best by the broken power-law model. A highly significant (99.9 per cent) emission line near 6.0 keV has been detected in the spectra of Mkn 766, Mkn 464, Mkn 290 and ESO 140–G43.

Key words: galaxies: Seyfert – X-rays: galaxies.

1 INTRODUCTION

X-ray spectroscopy of Seyfert galaxies obtained from *EXOSAT* and *Ginga* has revealed many interesting results (Turner & Pounds 1989; Pounds 1989; Turner et al. 1989). First, the spectral indices of the power-law spectra have a Gaussian distribution with mean energy index $\alpha = 0.7$ and intrinsic standard deviation $\sigma_\alpha = 0.2$. Secondly, in many of the spectra there is a soft excess and low-energy absorption. Thirdly, Fe *K*-shell emission and absorption lines are also common (Pounds et al. 1990), although not all Seyfert galaxies display all of these characteristics. Thus it is important to study more such objects in order to understand the nature of the active nucleus and its environment. In this paper we present spectral information on eight Seyfert galaxies (ESO 012–G21, Mkn 352, Mkn 374, Mkn 766, Mkn 279, Mkn 464, Mkn 290 and ESO 140–G43) which were observed with *EXOSAT*.

From analysis of the *EXOSAT* spectra of these galaxies we report, for the first time, the detection of soft excesses in seven of them (ESO 012–G21, Mkn 352, 374, 766, 279, 464 and 290) and the detection of iron emission lines in the spectra of Mkn 766, 464, 290 and ESO 140–G43.

Brief information about the individual galaxies is given below.

1.1 ESO 012–G21

This is a type 1 Seyfert galaxy (West 1979) with $m_V = 14.73$, $M = -21.6$, $B-V = 0.57$, $U-B = -0.25$ and $z = 0.031$ (West, Grosbol & Sterken 1980). X-ray detection with *Uhuru* (3U 0055 – 79) was doubtful (Giacconi et al. 1974), but the galaxy was detected with *Ariel V* (Bell Burnell & Chiappetti 1984). The first X-ray (2–10 keV) spectrum was obtained with the MSSL proportional counter spectrometer on *Ariel V* (Hayes, Culhane & Bell Burnell 1980), and it was observed later with *EXOSAT* by D. Molteni in the 0.1–10 keV range.

1.2 Mkn 352

Mkn 352 is a type 1 Seyfert galaxy ($m_V = 14.81$, $M = -20$, $B-V = 0.44$, $U-B = -0.66$ and $z = 0.015$; Markarian & Lipovetski 1971; Osterbrock 1977). It was observed with *Einstein* in the 0.2–4 keV range (Kriss, Canizares & Ricker 1980; Urry et al. 1989). The first X-ray observation beyond

4 keV was by H. Fink with *EXOSAT* in the 0.1–10 keV range but is not yet published.

1.3 Mkn 374

No spectral information in the X-ray region, except for the *Einstein* Imaging Proportional Counter (0.2–4 keV) results (Urry et al. 1987), is available for this Seyfert 1 galaxy ($m_V = 14.61$, $M = -22.5$, $B-V = 0.7$, $U-B = -0.38$; Markarian & Lipovetski 1971; Weedman 1973; Osterbrock 1977). The *EXOSAT* spectrum (0.1–10 keV) obtained by J. Bergeron on 1984 November 5 has not been published.

1.4 Mkn 766

Prior to the *EXOSAT* observations of this Seyfert 1 galaxy ($m_V = 14.0$, $M = -20.4$, $z = 0.012$; Markarian & Lipovetski 1976; Denisyuk & Lipovetski 1977), the only X-ray observation was with the *Einstein* IPC (Kriss et al. 1980; Urry et al. 1987). It was observed with *EXOSAT* at five epochs between 1985/363 and 1985/365, but the results have not been published.

1.5 Mkn 279

Mkn 279 (MCG 12-13-22; 3A 1348+700) is a type 1 Seyfert galaxy ($m_V = 14.46$, $M = -21.9$, $B-V = 0.69$, $U-B = -0.45$, $z = 0.031$; Walker & Chincarini 1967; Markarian 1969; Arakelian et al. 1971). Infrared (Lonsdale et al. 1985) and weak radio (de Bruyn & Wilson 1976; Ulvestad & Wilson 1984) emission has been detected. Prior to *EXOSAT*, X-ray observations were made with *Uhuru* (Tananbaum et al. 1978), *Ariel V* (Cooke et al. 1978; Elvis et al. 1978; Stark, Bell Burnell & Culhane 1978; McHardy et al. 1981; Bell Burnell & Chiappetti 1984), *HEAO-1* (Dower et al. 1980; Tennant & Mushotzky 1983; Mushotzky 1984; Wood et al. 1984; Reichert et al. 1985) and *Einstein* (Kriss & Doxsey 1983; Reichert et al. 1985; Urry et al. 1989). It was observed with *EXOSAT* at two epochs between 1983 and 1984 by S. J. Bell Burnell, but no spectra have yet been published. From an analysis of these spectra we have detected variable soft excesses which will be discussed in Section 3.

1.6 Mkn 464

By spectroscopy, Denisyuk & Lipovetski (1974) classified Mkn 464 as a type 1 Seyfert galaxy ($m_V = 16.1$, $M = -21.3$ and $z = 0.051$; Markarian & Lipovetski 1972; Denisyuk & Lipovetski 1974). Weak radio emission (~ 0.006 Jy) was detected by Ulvestad & Wilson (1984). X-ray observations were made with *HEAO-1* (Marshall et al. 1979; Dower et al. 1980; Tennant & Mushotzky 1983), *Ariel V* (Hayes, Culhane & Bell Burnell 1980) and *EXOSAT* (S. J. Bell Burnell).

1.7 Mkn 290

This type 1 Seyfert galaxy ($m_V = 14.96$, $B-V = 0.6$, $U-B = -0.62$, $z = 0.029$ and $M = -21.3$; Markarian 1969; Arakelian et al. 1971; Weedman 1973) was detected with *HEAO-1* (Wood et al. 1984) and spectra were obtained with *Einstein* (Kriss et al. 1980; Kruper, Urry & Canizares 1990) and *EXOSAT* (Turner & Pounds 1989).

1.8 ESO 140–G43

ESO 140–G43 (Fairall 51, Fairall 1977) is a compact *IRAS* Seyfert 1 galaxy ($m_V = 14.1$, $B-V = 0.73$, $U-B = -0.17$, $z = 0.014$ and $M = -20.5$; West, Dank & Alcaino 1978; Simkin, Su & Schwarz 1980; Osterbrock & De Robertis 1985; De Grijp et al. 1985; Glass 1985). To our knowledge, no X-ray spectra have previously been obtained for this Seyfert galaxy; the *EXOSAT* observation was carried out by D. Molteni.

2 OBSERVATIONS

EXOSAT observations were carried out with low- and medium-energy (LE and ME) detectors. The LE observations used Lexan 3000 (LX3) and aluminium/parylene (Al/P) filters (for details, see de Korte et al. 1981). The XANADU (X-ray Analysis and Data Utilization) software package was used to convert the background-subtracted LE count rates to obtain the LE pulse-height (PHA) spectra. Eight argon-filled proportional counters were used as detectors (Turner et al. 1981) to obtain the ME spectra. These detectors were divided into two groups of four, which could either be aligned with the pointing axis or offset by up to 2° to obtain background emissions. The ME observation mode for the galaxies (except for the observation of Mkn 279 on 1984/028) was with the two detector groups offset to obtain simultaneous background data, which were used to eliminate background effects from the source data. Background-subtracted LE and ME spectra of the above sources were obtained from the *EXOSAT* data base. A log of the LE and ME observations and the corresponding count rates appears in Table 1.

3 ANALYSIS OF LE AND ME SPECTRA

The LE and ME spectra were analysed with the XSPEC (X-ray Spectral Fitting) software package. A simple power-law and uniform-absorption model (model 1) was used to fit the spectra, with the effective photoelectric cross-sections given by Morrison & McCammon (1983). The parameters of the fit of this model are presented in Table 2. The χ^2 statistics (using χ^2 minimization) suggest that the fit is acceptable, although the values of the hydrogen column densities (N_H) for all the galaxies, except ESO 140–G43, are smaller than the corresponding galactic N_H values. (Since we do not know the galactic N_H values towards ESO 021–G21 and 140–G43, we have assumed N_H to be 2.0×10^{20} cm^{-2} for these objects.) Thus, in the next model, we have frozen the values of N_H with the corresponding galactic values. The best-fitting parameters of the power-law and fixed-absorption model (model 2) are shown in Table 3 along with the 90 per cent confidence errors computed as described by Lampton, Margon & Bowyer (1976) ($\chi^2_{min} + 4.61$ for two free parameters). The reduced χ^2 (χ^2_r) values in Table 3 are large (> 1.0) and show that this model is unacceptable. The photon spectra are presented in Figs 1(a)–(h) along with the power-law plus absorption model convolved through the detector response. Residuals between the model and the spectra are shown in the lower panels of these figures.

Table 1. Log of observations of the LE and ME spectra and count rates of eight Seyfert galaxies.

Source	Start time	End time	LE count rate (10^{-4} cm^{-2} s^{-1})			ME count rate* (10^{-3} cm^{-2} s^{-1})
	D H M	D H M	(LX3)	(Al/P)	(B)	
ESO 012-G21	1985/108 09 12	108 12 49	1.85±0.24	0.69±0.15		0.61±0.06
Mkn 352	1983/319 02 46	319 03 47	0.37±0.05	0.28±0.07		1.34±0.12
Mkn 374	1984/310 18 44	311 02 13	0.22±0.03			0.59±0.04
$ Mkn 766	1985/363 18 17	364 04 02	2.65±0.23			3.10±0.09
$ Mkn 766	1985/364 04 16	364 13 27	2.30±0.21			2.70±0.08
$ Mkn 766	1985/364 13 45	365 00 57	1.95±0.19			2.43±0.07
$ Mkn 766	1985/365 01 04	365 11 19	2.88±0.23			3.01±0.08
$ Mkn 766	1985/365 11 36	366 00 08	3.45±0.26			3.80±0.07
Mkn 279	1983/320 16 52	320 20 48	1.32±0.11	0.51±0.06	0.11±0.02	2.17±0.09
+ Mkn 279	1984/028 18 29	028 21 47	1.20±0.08	0.55±0.04	0.13±0.02	1.78±0.11
Mkn 464	1985/178 23 21	199 04 30	5.26±0.46	2.31±0.19		1.04±0.05
$ Mkn 290	1986/056 00 05	056 07 01	4.43±0.32	2.10±0.29		0.75±0.04
ESO 140-G43	1985/105 13 30	105 16 22	1.29±0.36			2.12±0.10

Notes: *the count rates are for PHA channels 6–35 corresponding to the energy range 2–10 keV with the best signal-to-noise ratio; $ Detector 3 was off during ME observations; + Only half of detector 2 was on during ME observations.

Already we have seen from the fitted parameters of model 1 (see Table 2) that the values of N_H, except for ESO 140–G43, are smaller than the corresponding galactic N_H values, which thus imply source spectra with more emission than the power-law predictions at low energies, i.e. a 'soft excess' (Wilkes & Elvis 1987; Kruper et al. 1990). It can also be seen from the contour plots by Wilkes & Elvis (1987) that forcing a column density in the presence of a soft excess always steepens the spectral slope. Comparison of models 1 and 2 (see Tables 2 and 3) also shows that the spectral slopes of model 2 are steeper than those obtained from model 1, thus suggesting that the soft excesses may be present in the spectra of ESO 012–G21, Mkn 352, 374, 766, 279, 464 and 290, and they may stand above the extrapolation of the hard (ME) power law. Results from fitting these spectra with the fixed power law (obtained from the fits to the ME data only) plus a fixed-absorption model (model 3) are given in Table 4. In Figs 2(a)–(g) we present the observed LE + ME spectra of these seven galaxies along with model 3 convolved through the detector response, and the corresponding residuals are in the lower panels. Fig. 3 shows the observed spectrum of ESO 140–G43 with model 1, and residuals of the five spectra of Mkn 766 are in Fig. 4. From the residuals in Figs 2 and 4, we find that the soft excesses are indeed present in the seven galaxies listed above, generally at more than the 3σ level (see Table 4). Any systematic errors due to inaccuracies in subtraction of the background could contribute no more than 30 to 40 per cent of the measured soft excesses.

To fit the soft excesses, two power-law, thermal bremsstrahlung (model 4) and broken power-law (model 5) models were tried. The two-power laws and the thermal bremsstrahlung (Table 5) did not fit the data well ($\chi^2_r \gg 1.0$). Only the broken power-law model (with the break energy fixed at 0.6 keV, following Wilkes et al. 1989) fits well with the spectra of the seven galaxies (see Table 6), but it is difficult to

Table 2. Model 1: power law + absorption.

Source	Date	α[a]	N[b]	N_H^c (observed)	N_H^c (galactic)	χ_r^2/d.o.f.
ESO 012–G21	1985/108	$0.21^{+0.18}_{-0.15}$	$0.80^{+0.62}_{-0.30}$	$0<0.50$	2.00[d]	1.10/30
Mkn 352	1983/319	$0.82^{+0.30}_{-0.28}$	$4.58^{+2.05}_{-1.43}$	$3.01^{+3.72}_{-1.88}$	5.60[e]	1.24/31
Mkn 374	1984/310	$0.80^{+0.26}_{-0.28}$	$1.95^{+0.80}_{-0.60}$	$2.00^{+2.37}_{-1.32}$	6.30[e]	1.18/29
Mkn 766	1985/363	$0.81^{+0.11}_{-0.12}$	$8.96^{+1.44}_{-1.25}$	$0<0.80$	1.60[f]	1.24/29
Mkn 766	1985/364	$0.98^{+0.13}_{-0.11}$	$11.77^{+1.79}_{-1.57}$	$0<1.80$	1.60[f]	1.34/27
Mkn 766	1985/364	$1.14^{+0.11}_{-0.12}$	$11.17^{+1.53}_{-1.40}$	$1.74^{+0.72}_{-0.54}$	1.60[f]	1.06/32
Mkn 766	1985/365	$0.95^{+0.10}_{-0.11}$	$10.30^{+1.40}_{-1.24}$	$0<1.05$	1.60[f]	1.25/32
Mkn 766	1985/365	$1.07^{+0.07}_{-0.07}$	$15.72^{+1.44}_{-1.34}$	$0<1.57$	1.60[f]	1.10/32
Mkn 279	1983/320	$0.84^{+0.09}_{-0.09}$	$6.90^{+0.84}_{-0.77}$	$1.10^{+0.50}_{-0.40}$	1.90[e]	1.48/34
Mkn 279	1984/028	$0.40^{+0.06}_{-0.04}$	$3.43^{+0.32}_{-0.20}$	0.00	1.90[e]	1.54/34
Mkn 464	1985/178	$0.33^{+0.09}_{-0.07}$	$1.69^{+0.60}_{-0.45}$	$0<0.30$	1.70[g]	1.32/26
Mkn 290	1986/056	$0.33^{+0.07}_{-0.05}$	$1.43^{+0.17}_{-0.09}$	$0<0.90$	1.80[e]	0.80/29
ESO 140–G43	1985/105	$0.46^{+0.21}_{-0.21}$	$4.28^{+1.49}_{-1.08}$	$11.00^{+17.8}_{-6.9}$	2.00[d]	0.70/28

Notes: [a]energy index; [b]normalization in 10^{-3} photon cm^{-2} s^{-1} keV^{-1} at 1 keV; [c]column density in 10^{-20} cm^{-2}; [d]assumed; [e]Stark et al. (in preparation); [f]Elvis et al. (1989); [g]Heiles (1975).

distinguish between these latter two models for the soft excess, because of the low signal-to-noise ratios. The best-fitting parameters of the thermal bremsstrahlung and broken power-law models are given in Tables 5 and 6, respectively.

It was noted in the Introduction that there is evidence for the presence of iron K-shell emission and absorption lines in the X-ray spectra of Seyfert galaxies (Pounds 1989; Leighly, Pounds & Turner 1989; Pounds et al. 1989, 1990; Ghosh & Soundararajaperumal 1991a,b and references therein), and the residuals in Figs 1(d) and 1(f)–(h) indeed indicate the presence of an emission feature near 6.0 keV. Thus a Gaussian component with fixed linewidth ($\sim$0.1 keV) and variable line-centre energy was added to the power-law plus fixed-absorption model and used to fit the spectra of Mkn 766, 464, 290 and ESO 140–G43. The best-fitting parameters of this model (model 6) with 90 per cent errors are given in Table 7. The χ^2 statistics suggest that the fit is better than with the power-law model. F-test calculations between the power-law (see Table 3) and the Gaussian-line (see Table 7) models show that the inclusion of the emission line is

Table 3. Model 2: power law + fixed absorption.†

Source	Date	α[a]	N	Flux[c] 0.1–2 (keV)	Flux[c] 2–10 (keV)	L_x[d] 0.1–2 (keV)	L_x[d] 2–10 (keV)	χ^2_r/d.o.f.
ESO 012–G21	1985/108	$0.87^{+0.13}_{-0.14}$	$1.89^{+0.26}_{-0.24}$	0.46 ± 0.06	0.58 ± 0.06	2.00 ± 0.26	2.50 ± 0.26	1.30/31
Mkn 352	1983/319	$1.03^{+0.12}_{-0.13}$	$5.95^{+0.78}_{-0.81}$	1.36 ± 0.18	1.46 ± 0.13	1.34 ± 0.18	1.43 ± 0.13	1.25/32
Mkn 374	1984/310	$1.16^{+0.13}_{-0.15}$	$3.11^{+0.46}_{-0.50}$	0.69 ± 0.09	0.62 ± 0.04	6.00 ± 0.78	5.39 ± 0.35	1.35/30
Mkn 766	1985/363	$1.06^{+0.07}_{-0.08}$	$12.30^{+1.00}_{-1.10}$	3.91 ± 0.34	2.88 ± 0.08	2.45 ± 0.21	1.80 ± 0.05	1.78/30
Mkn 766	1985/364	$1.06^{+0.05}_{-0.07}$	$12.76^{+0.90}_{-0.93}$	4.05 ± 0.37	3.02 ± 0.09	2.54 ± 0.23	1.89 ± 0.06	1.34/28
Mkn 766	1985/364	$1.11^{+0.06}_{-0.06}$	$10.88^{+0.76}_{-0.79}$	3.53 ± 0.34	2.34 ± 0.07	2.22 ± 0.21	1.48 ± 0.04	1.02/33
Mkn 766	1985/365	$1.14^{+0.06}_{-0.07}$	$12.95^{+0.91}_{-0.95}$	4.24 ± 0.34	2.71 ± 0.07	2.66 ± 0.21	1.70 ± 0.04	1.59/33
Mkn 766	1985/365	$1.13^{+0.04}_{-0.05}$	$16.91^{+0.95}_{-0.97}$	5.52 ± 0.42	3.58 ± 0.07	3.46 ± 0.26	2.24 ± 0.04	1.16/33
Mkn 279	1983/320	$0.95^{+0.05}_{-0.05}$	$7.90^{+0.50}_{-0.50}$	2.34 ± 0.19	2.20 ± 0.09	9.97 ± 0.81	9.37 ± 0.38	1.64/35
Mkn 279	1984/028	$1.04^{+0.05}_{-0.06}$	$7.69^{+0.45}_{-0.44}$	2.34 ± 0.19	1.87 ± 0.11	9.97 ± 0.68	7.97 ± 0.47	1.67/35
Mkn 464	1985/178	$1.12^{+0.06}_{-0.07}$	$4.66^{+0.33}_{-0.34}$	1.20 ± 0.10	1.00 ± 0.05	14.1 ± 1.20	11.8 ± 0.60	1.50/27
Mkn 290	1986/056	$1.18^{+0.07}_{-0.08}$	$4.14^{+0.31}_{-0.32}$	0.91 ± 0.06	0.90 ± 0.05	3.40 ± 0.22	3.40 ± 0.20	1.65/30
ESO 140–G43	1985/105			0.80 ± 0.20	2.55 ± 0.12	0.70 ± 0.17	2.20 ± 0.10	

Notes: †fixed with corresponding N_H value; [a]energy index; [b]normalization in 10^{-3} photon cm^{-2} s^{-1} keV^{-1} at 1 keV; [c]flux in 10^{-11} erg cm^{-2} s^{-1}; [d]luminosity in 10^{43} erg s^{-1}.

highly significant (> 99.9 per cent). Measured equivalent widths are also given in Table 7. Only the statistical errors have been considered, in order to compute the errors in the equivalent widths. Figs 5(a)–(d) display the incident spectra of the four galaxies along with the Gaussian-line (model 6) convolved through the detector response, and the corresponding residuals are shown in the lower panels of each figure.

4 RESULTS

4.1 ESO 012–G21

For the first time, *EXOSAT* results have detected the presence of a soft excess in the spectrum of ESO 012–G21 (see Table 4 and Fig. 2a). This soft excess fits well with the broken power-law model, which indicates that two components (soft and hard) are required to fit the spectrum.

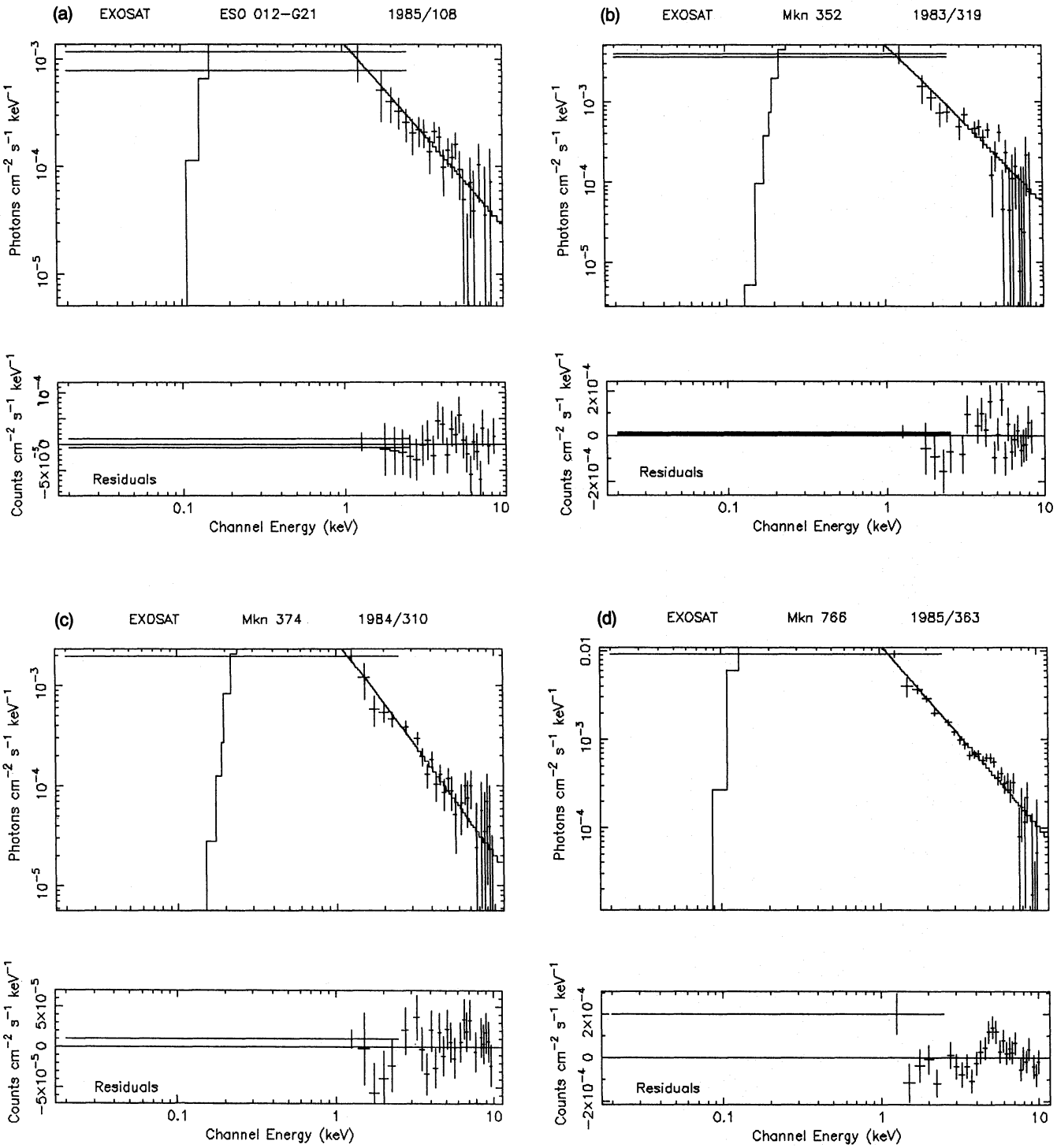

Figure 1. Incident photon spectra of the Seyfert galaxies (a) ESO 012−G21, (b) Mkn 352, (c) Mkn 374, (d) Mkn 766, (e) Mkn 279, (f) Mkn 464, (g) Mkn 290, and (h) ESO 140−G43. The spectra have been fitted with a simple power-law and fixed-absorption model. The lower panel of each part shows the residuals between the spectrum and the model.

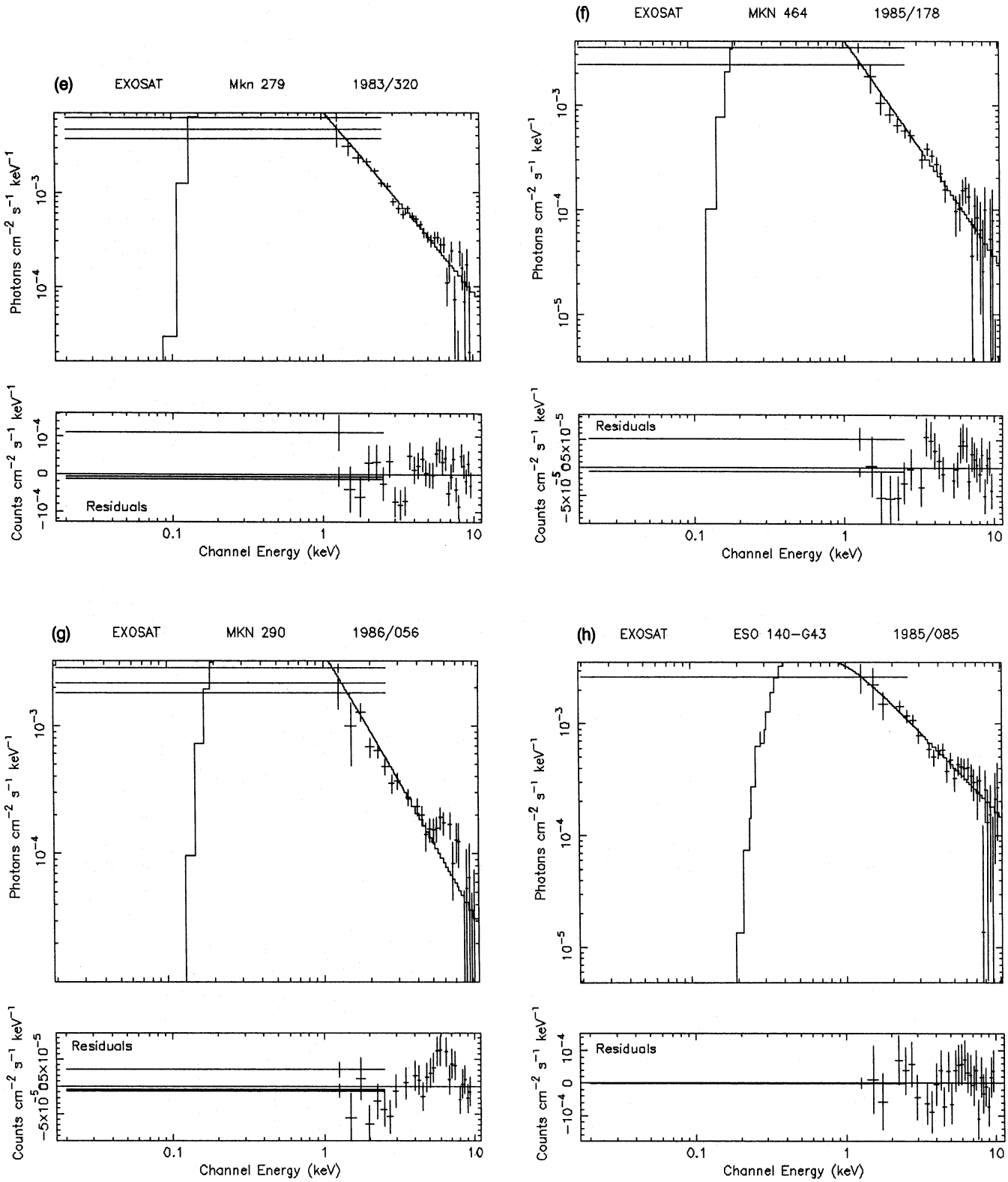

Figure 1 – *continued*

Table 4. Model 3: fixed power law* + fixed absorption.

Source	Date	α [a]	N [b]	N_H [c]	Soft excess [d]	χ^2_r/d.o.f
ESO 012 -G21	1985/108	0.43	0.63	2.00	0.50±0.10	2.03/32
Mkn 352	1983/319	0.66	4.03	5.60	0.70±0.20	2.07/33
Mkn 374	1984/310	0.63	1.61	6.30	0.58±0.10	2.38/31
Mkn 766	1985/363	0.83	9.55	1.60	5.30±0.90	2.39/31
Mkn 766	1985/364	0.99	$11.93^{+0.43}_{-0.42}$	1.60	3.60±0.80	1.48/29
Mkn 766	1985/364	0.85	$8.08^{+0.43}_{-0.40}$	1.60	3.40±0.80	1.98/34
Mkn 766	1985/365	0.95	10.54	1.60	5.10±0.90	2.18/34
Mkn 766	1985/365	1.07	$15.81^{+0.74}_{-0.56}$	1.60	5.40±1.00	1.21/34
Mkn 279	1983/320	0.80	6.70	1.90	2.20±0.50	2.11/36
Mkn 279	1984/028	0.80	6.60	1.90	1.80±0.40	2.84/36
Mkn 464	1985/178	0.76	$3.10^{+0.18}_{-0.11}$	1.70	0.60±0.10	1.44/28
Mkn 290	1986/056	0.55	2.20	2.00	1.00±0.14	2.95/31

Notes: *obtained from the fits to the ME data only; [a]energy index; [b]normalization in 10^{-3} photon cm^{-2} s^{-1} keV^{-1} at 1 keV; [c]galactic column density in 10^{-20} cm^{-2}; [d]counts in 10^{-4} cm^{-2} s^{-1} keV^{-1}.

However, the spectrum from *Ariel V* observations fitted best with the single power-law model ($\alpha = 0.80$, Hayes et al. 1980). The hard X-ray (2–10 keV) flux of this source decreased by a factor of ~7 between 1976 August ($F_{2-10} \sim (3.8 \pm 0.6) \times 10^{-11}$ erg cm^{-2} s^{-1}, *Ariel V* observation) and 1985 April ($F_{2-10} \sim (0.58 \pm 0.06) \times 10^{-11}$ erg cm^{-2} s^{-1}, *EXOSAT* observation). The derived plasma temperature, obtained from the fits of the thermal bremsstrahlung model, is $\sim 4.6^{+2.5}_{-1.3}$ keV.

4.2 Mkn 352

From comparison of the soft fluxes (0.2–4 keV) measured with *Einstein* [$(3.34 \pm 0.05) \times 10^{-11}$ erg cm^{-2} s^{-1}; Kruper et al. 1990] and *EXOSAT* [$(2.0 \pm 0.15) \times 10^{-11}$ erg cm^{-2} s^{-1}], it appears that the luminosity did not vary significantly between 1980 January and 1983 November. Fig. 2(b) shows that the soft excess stands above the extrapolation of the hard (ME) power law (see Table 4). The thermal bremsstrahlung model also fits well with the spectra of this galaxy, and the derived plasma temperature is $\sim 3.6^{+1.6}_{-0.9}$ keV.

4.3 Mkn 374

The X-ray (0.2–4 keV) luminosity did not vary significantly between the *Einstein* [$(0.7 \pm 0.05) \times 10^{-11}$ erg cm^{-2} s^{-1} measured on 1979 April; Kruper et al. 1990 and references therein] and *EXOSAT* [$(0.98 \pm 0.06) \times 10^{-11}$ erg cm^{-2} s^{-1} measured on 1984 November] observations. There is a weak soft excess in the spectrum (see Fig. 2c) and the value of α_1 is larger than α_2 as obtained from the broken power-law fits (see Table 6).

4.4 Mkn 766

The LE and ME count rates, obtained with *EXOSAT* between 1985/363 and 1985/365, are plotted in Fig. 6. Table 1 and Fig. 6 show that the LE and ME fluxes varied by 32 and 20 per cent, respectively, within 11 h. Also it can be seen from Fig. 7 that the LE and ME variations are correlated (the linear correlation coefficient is 0.97 for five observations which suggests that the probability of the fit being random is 0.5 per cent). The soft excess detected in this ultrasoft excess source (Urry et al. 1989) has displayed weak variability on a time-scale of hours (see Fig. 4) and is correlated with the variations of the LE and ME fluxes, the linear correlation coefficients being 0.87 and 0.84, respectively (see Fig. 8), the soft excess being stronger when the galaxy was brighter. This type of correlated variability has already been seen in other Seyfert galaxies, such as NGC 3783 (Ghosh et al. 1991), 3C 382 (Ghosh & Soundararajaperumal 1992), MCG 2-58-22, etc, but is not understood.

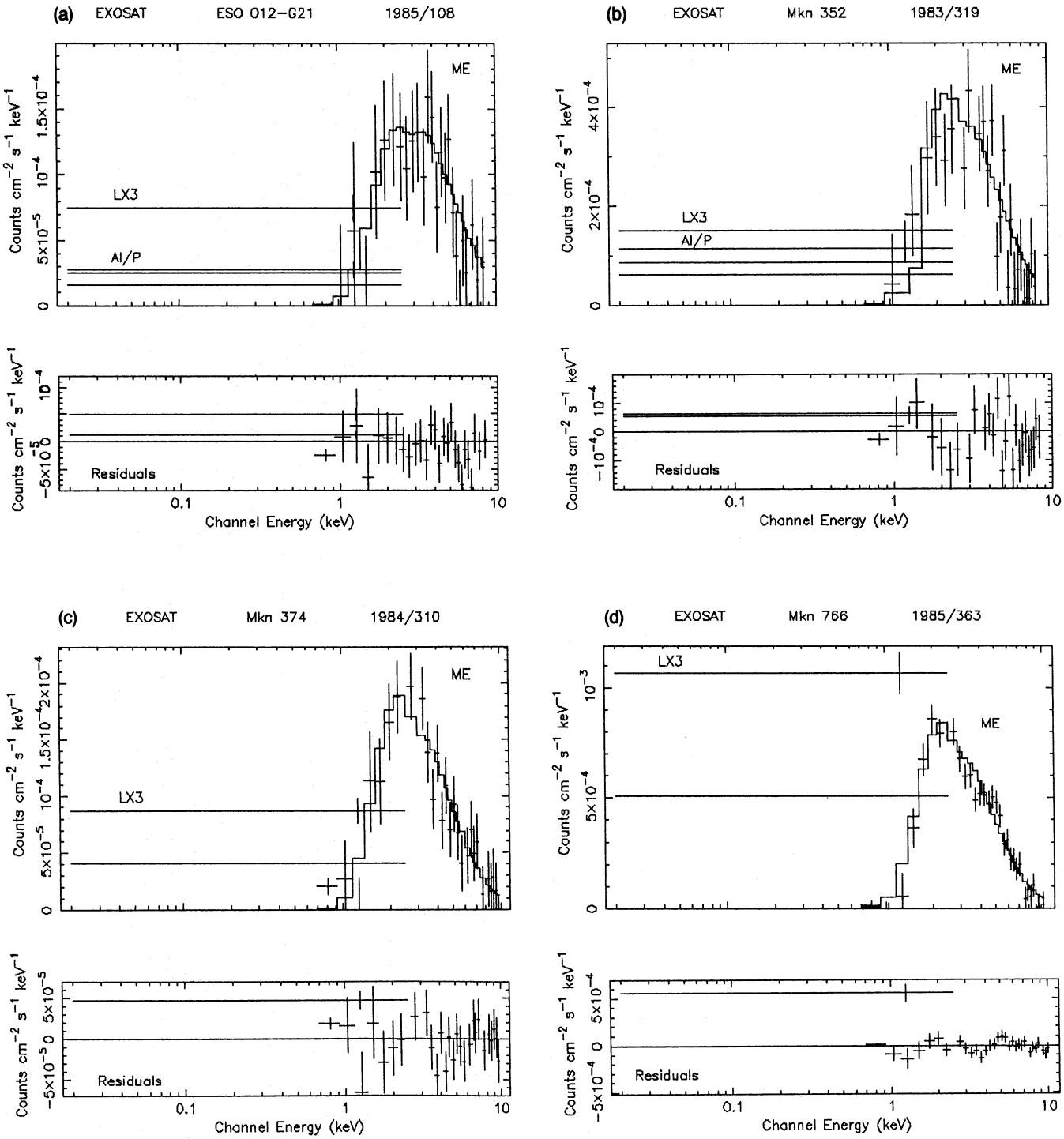

Figure 2. Observed X-ray (0.1–10 keV) spectrum of (a) ESO 012–G21, (b) Mkn 352, (c) Mkn 374, (d) Mkn 766, (e) Mkn 279, (f) Mkn 464, and (g) Mkn 290. Also shown for each spectrum is the fixed power-law (obtained from the fits to the ME data only) + fixed-absorption (fixed with the galactic hydrogen column density value) model convolved through the detector response. The lower panel of each figure displays the residuals between the spectrum and the model in units of counts.

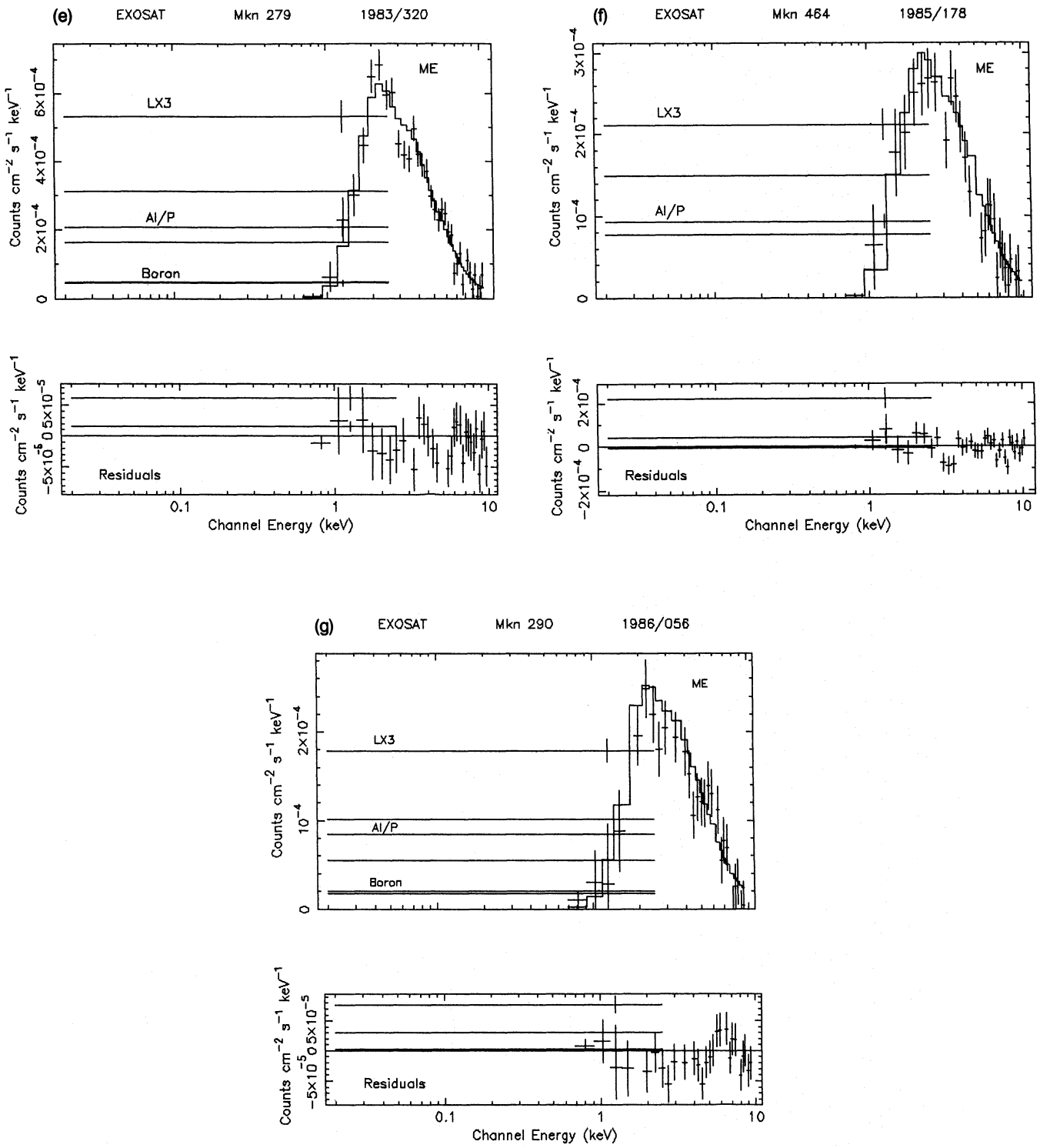

Figure 2 – *continued*

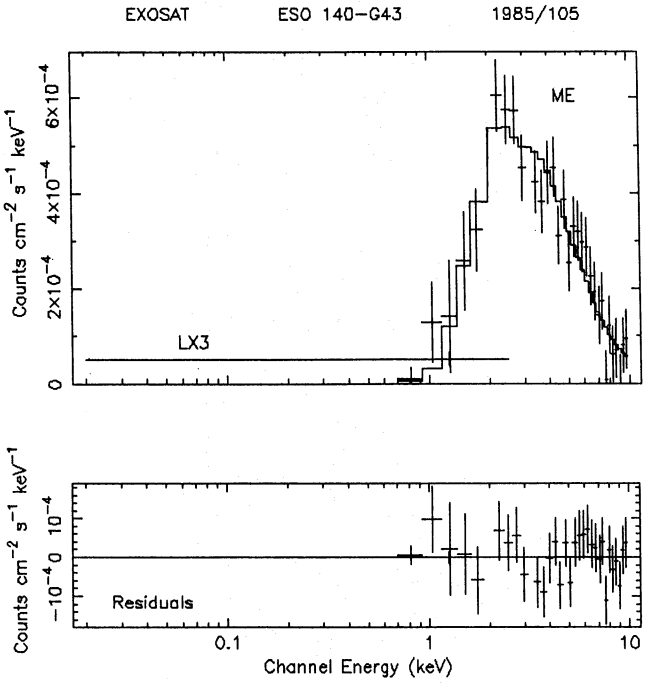

Figure 3. Observed X-ray (0.1–10 keV) spectrum of ESO 140–G43 along with the power-law + absorption model convolved through the detector response. The lower panel of the figure displays the residuals between the spectrum and the model in units of counts.

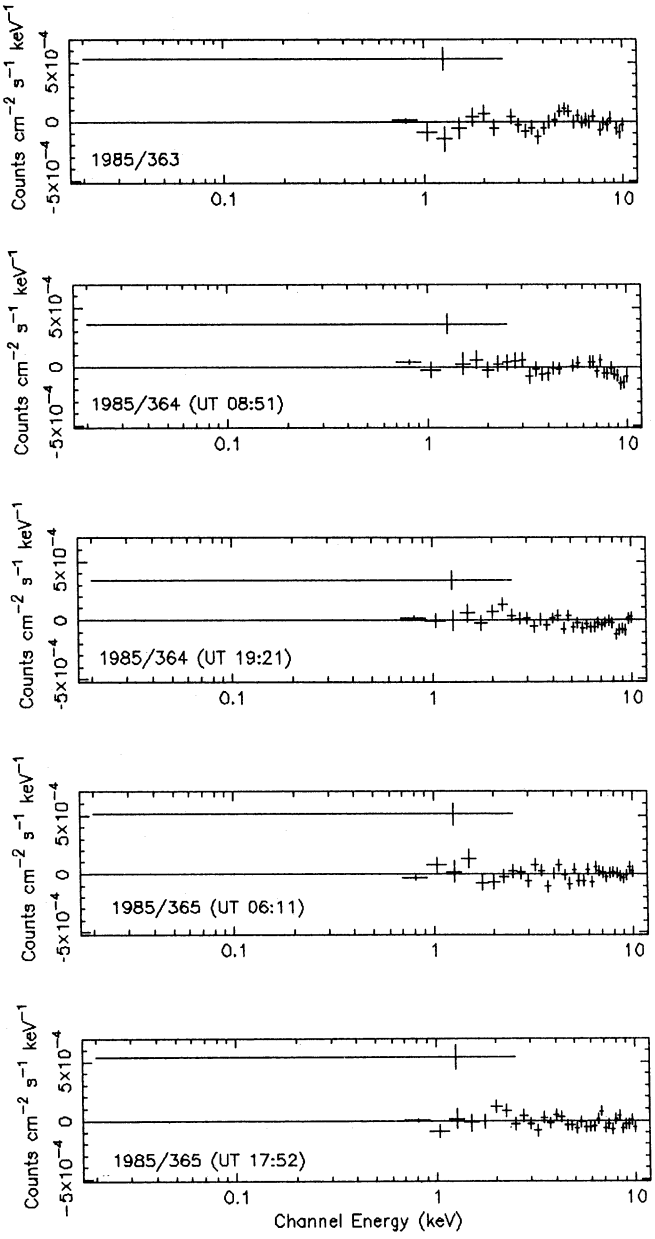

Figure 4. Residuals between different spectra of Mkn 766 and model 3.

4.5 Mkn 279

The X-ray fluxes in the soft and hard X-ray bands, obtained from *Uhuru*, *Ariel V*, *Einstein*, *HEAO-1* and *EXOSAT*, indicate that this galaxy has displayed no marked variations of X-ray luminosity on a time-scale of years or months. In addition, the soft excess values [(2.2 ± 1.0) and $(1.8 \pm 0.4) \times 10^{-4}$ count cm^{-2} s^{-1} keV^{-1}], measured from the spectral fits (Fig. 2e), were almost unchanged between 1983/320 and 1984/028. This soft excess is best explained by the broken power-law model (see Table 6).

4.6 Mkn 464

The X-ray flux measured by *Ariel V* on 1977 January in the 2–10 keV band was $(2.7 \pm 0.5) \times 10^{-11}$ erg cm^{-2} s^{-1} (Hayes et al. 1980), while the fluxes from *HEAO-1* on 1977 December (Marshall et al. 1979) and 1978 October (Dower et al. 1980) were (2.6 ± 0.5) and $(0.8 \pm 0.4) \times 10^{-11}$ erg cm^{-2} s^{-1}, respectively. The 2–10 keV flux thus decreased by a factor of 3 between 1977 December and 1978 October, although there was no variation between 1978 October (*HEAO-1* observation) and 1985 June (*EXOSAT* observation). *Ariel V* detected a steep spectral index ($\alpha = 2.0$) and high $N_{\rm H}$ ($\sim 2.5 \times 10^{23}$ cm^{-2}) in the 2–10 keV range (Hayes et al. 1980), and the values from *HEAO-1* in the 2–40 keV range were $\alpha = 0.39^{+0.19}_{-0.11}$ and $N_{\rm H} \sim (0\text{–}0.9) \times 10^{22}$ cm^{-2} (Mushotzky 1984), whereas from the *EXOSAT* results we found no low-energy absorption in this galaxy. The *EXOSAT* results indeed reveal the presence of a soft excess and the values of the soft and hard spectral indices are 2.83 ± 0.60 and 0.76 ± 0.18, respectively (Table 6). The residuals of Fig. 1(f) show emission features at 3 and 6 keV, but it is not clear whether these features are intrinsic to the source or background-induced artefacts. The fact that the $\chi^2_{\rm r}$ value reduced significantly when the Gaussian-line component was added to the power-law model (see Tables 3 and 7) suggests that the emission line at 6 keV is real.

4.7 Mkn 290

The *EXOSAT* spectrum was analysed, using a single power law, by Turner & Pounds (1989) and the derived values of α

Table 5. Model 4: thermal bremsstrahlung + fitted absorption.†

Source	Date	kT[a]	N[b]	χ^2_r /d.o.f.
ESO 012 -G21	1985/108	$4.56^{+2.47}_{-1.29}$	$1.01^{+0.37}_{-0.31}$	1.14/31
Mkn 352	1983/319	$3.60^{+1.57}_{-0.90}$	$3.74^{+1.58}_{-1.20}$	1.75/32
Mkn 374	1984/310	4.26	1.33	2.14/30
Mkn 766	1985/363	6.30	3.95	4.00/30
Mkn 766	1985/364	4.43	5.82	3.30/28
Mkn 766	1985/364	3.83	5.48	2.14/33
Mkn 766	1985/365	4.92	4.83	4.13/33
Mkn 766	1985/365	4.44	7.10	3.92/33
Mkn 279	1983/320	5.32	3.44	3.76/35
Mkn 279	1984/028	2.34	8.40	3.65/35
Mkn 464	1985/178	2.96	3.08	2.29/27
Mkn 290	1986/056	3.47	2.25	3.25/30
ESO 140 -G43	1985/105	$98.23^{+7.60}_{-4.20}$	0.77	0.90/29

Notes: †fixed with corresponding galactic N_H value; [a]plasma temperature in keV; [b]normalization in 10^{-3} photons $cm^{-2}\,s^{-1}\,keV^{-1}$ at 1 keV.

and N_H are $0.73^{+0.30}_{-0.14}$ and $(0.1-0.3)\times10^{21}$ cm^{-2} respectively. We have detected a soft excess and an emission line (see Figs 2g and 5c). From a comparison of the X-ray fluxes obtained with *Einstein* (Kruper et al. 1990) and *EXOSAT*, we find no significant variation between 1979/210 and 1985/055.

4.8 ESO 140–G43

This is a flat-spectrum ($\alpha = 0.46 \pm 0.21$) source with a weak low-energy absorption (see Table 2). No soft excess is present, but there is an emission line at about 6.0 keV.

5 DISCUSSION

Spectral analysis of the eight Seyfert galaxies shows that the seven galaxies ESO 012–G21, Mkn 352, 374, 766, 279, 464 and 290 have soft excesses in their spectra with no low-energy absorption, but no soft excess was found in ESO 140–G43 in which low-energy absorption was detected. Probably ESO 140–G43 also has a weak soft excess, which was hidden by its $N_H \sim 10^{21}$ cm^{-2} absorber. Thus we suggest that soft excesses are a common feature of Seyfert galaxies and the detection of soft excess depends on the low-energy absorption in the line of sight to the source.

Measured line-centre energies of the Gaussian line detected in the X-ray spectra of Mkn 766, 464, 290 and ESO 140–G43 are consistent, considering the uncertainties, with the redshifted 6.4-keV fluorescent iron line or the 6.7-keV helium-like iron line. Because of the poor resolution of the ME detectors (FWHM at 6 keV is ~1.2 keV), it is difficult to determine, from the measured line-centre energies, the origin of the emission lines, the equivalent widths of which are larger than the values usually found in Seyfert galaxies (Pounds 1989; Pounds et al. 1989 and references therein). For the strong sources, which are mainly galactic, it has been found that the Fe *K*-line equivalent widths deter-

Table 6. Model 5: broken power law* + fixed absorption.†

Source	Date	α_1 [a]	α_2 [a]	N [b]	χ^2_r /d.o.f.
ESO 012 -G21	1985/108	$3.47^{+0.97}_{-1.13}$	$0.25^{+0.34}_{-0.35}$	$0.16^{+0.36}_{-0.11}$	1.06/30
Mkn 352	1983/319	$2.30^{+1.16}_{-1.68}$	$0.81^{+0.30}_{-0.30}$	$2.10^{+6.00}_{-1.42}$	1.23/31
Mkn 374	1984/310	$3.17^{+0.95}_{-1.18}$	$0.81^{+0.27}_{-0.27}$	$0.60^{+1.09}_{-0.23}$	1.18/29
Mkn 766	1985/363	$1.90^{+0.30}_{-0.30}$	$0.81^{+0.11}_{-0.12}$	$5.17^{+2.13}_{-1.47}$	1.23/29
Mkn 766	1985/364	$1.28^{+0.32}_{-0.35}$	$0.99^{+0.12}_{-0.11}$	$10.15^{+4.35}_{-2.95}$	1.34/27
Mkn 766	1985/364	$2.04^{+0.33}_{-0.39}$	$0.85^{+0.10}_{-0.12}$	$11.69^{+4.88}_{-3.31}$	1.02/32
Mkn 766	1985/365	$1.76^{+0.26}_{-0.28}$	$0.94^{+0.11}_{-0.09}$	$6.85^{+2.40}_{-1.76}$	1.25/32
Mkn 766	1985/365	$1.40^{+0.20}_{-0.25}$	$1.07^{+0.07}_{-0.07}$	$13.40^{+3.30}_{-2.60}$	1.09/32
Mkn 279	1983/320	$1.51^{+0.31}_{-0.33}$	$0.83^{+0.09}_{-0.10}$	$4.81^{+1.76}_{-1.26}$	1.48/34
Mkn 279	1984/028	$1.74^{+0.42}_{-0.46}$	$0.80^{+0.17}_{-0.17}$	$3.63^{+2.34}_{-1.45}$	1.54/34
Mkn 464	1985/178	$2.83^{+0.55}_{-0.63}$	$0.76^{+0.18}_{-0.18}$	$1.00^{+0.86}_{-0.45}$	1.05/26
Mkn 290	1986/056	$3.12^{+0.51}_{-0.54}$	$0.65^{+0.18}_{-0.19}$	$0.63^{+0.50}_{-0.28}$	0.75/29

Notes: *break energy fixed at 0.6 keV; †fixed with corresponding galactic N_H value; [a]energy index; [b]normalization in 10^{-3} photon cm^{-2} s^{-1} keV^{-1} at 1 keV.

Table 7. Model 6: power law + absorption + Gaussian line.

Source	Date	α [a]	N [b]	N_H [c]	E_L [d]	E_N [e]	EW [f]	χ^2_r /d.o.f.
Mkn 766	1985/363	$1.17^{+0.06}_{-0.07}$	$12.76^{+0.91}_{-0.95}$	1.60*	$5.20^{+0.24}_{-0.23}$	$3.21^{+0.95}_{-0.95}$	371±110	0.82/28
Mkn 766	1985/364	$1.10^{+0.05}_{-0.08}$	$12.94^{+0.86}_{-0.90}$	1.60*	$6.10^{+0.52}_{-0.58}$	$2.42^{+1.47}_{-1.44}$	357±214	1.15/26
Mkn 464	1985/178	$1.19^{+0.08}_{-0.08}$	$4.59^{+0.30}_{-0.30}$	1.70*	$6.43^{+0.90}_{-0.77}$	$0.85^{+0.72}_{-0.70}$	524±437	1.20/25
Mkn 290	1986/056	$1.28^{+0.07}_{-0.08}$	$4.12^{+0.29}_{-0.30}$	1.80*	$6.05^{+0.30}_{-0.31}$	$2.12^{+0.66}_{-0.66}$	424±132	0.72/28
ESO 140 -G43	1985/105	$0.67^{+0.29}_{-0.26}$	$5.42^{+2.43}_{-1.59}$	$17.0^{+24.0}_{-10.0}$	$6.00^{+0.55}_{-0.47}$	$2.10^{+1.48}_{-1.43}$	354±244	0.50/26

Notes: *fixed with corresponding galactic N_H value; [a]energy index; [b]normalization in 10^{-3} photon cm^{-2} s^{-1} keV^{-1} at 1 keV; [c]column density in 10^{20} cm^{-2}; [d]line energy in keV; [e]line intensity in 10^{-4} photon cm^{-2} s^{-1}; [f]equivalent width in eV.

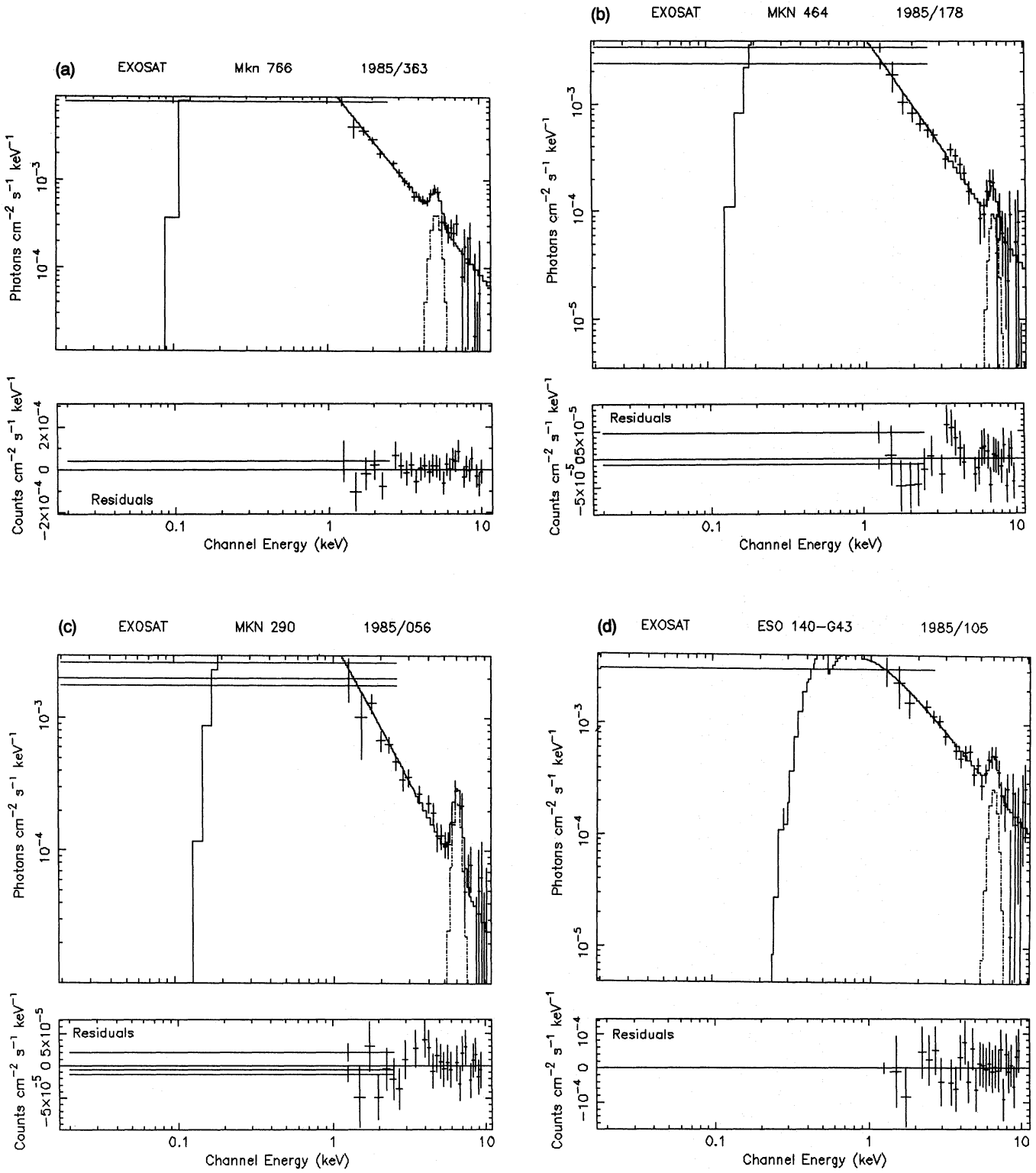

Figure 5. Incident photon spectra of the Seyfert galaxies (a) Mkn 766, (b) Mkn 464, (c) Mkn 290, and (d) ESO 140−G43, fitted with power-law + fixed-absorption + Gaussian-line models. The lower panel of each figure shows the residuals between the spectrum and the model.

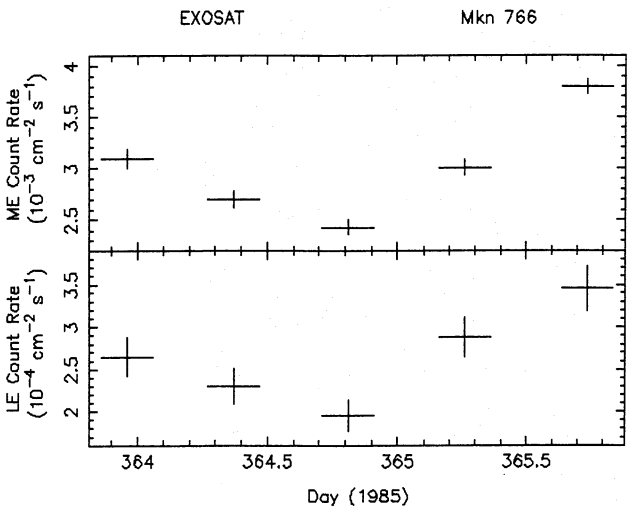

Figure 6. Plot of the LE and ME count rates of Mkn 766 versus the date of observations.

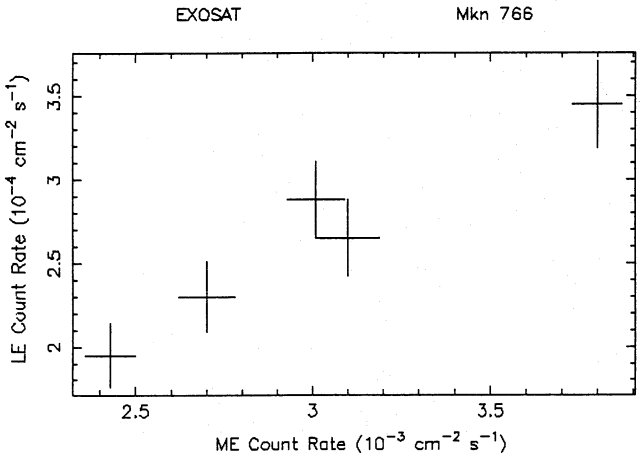

Figure 7. Observed count rates of the LE versus ME of Mkn 766.

mined from *EXOSAT* data are consistent with those determined from *Ginga* spectra, whereas the Fe *K*-line equivalent widths determined from *EXOSAT* spectra for weak sources are significantly and systematically higher than those determined from the *Ginga* data. This is because of statistical fluctuations in the flux at the line energy which will result in a large line flux giving a large equivalent width. Thus the measured equivalent widths of the iron *K* line in Mkn 766, 464, 290 and ESO 140–G43 cannot be used to determine uniquely the origin of the line.

A large equivalent width indicates that an emission line may be thermal in origin and the corresponding thermal emission at $\sim 10^{43}$–10^{44} erg s^{-1} corresponds to that from a rich cluster. No X-ray clusters have been detected near Mkn 766, 464, 290 and ESO 140–G43, which suggests that a thermal origin of the iron line in these four galaxies is very unlikely. It may be due to the fluorescence of cold iron, but the amount of cold matter required to produce the line would be larger than $\sim 5 \times 10^{22}$ cm^{-2} which we would not be able to detect in the lines of sight to these sources. Thus the detection of iron *K* lines with relatively larger equivalent

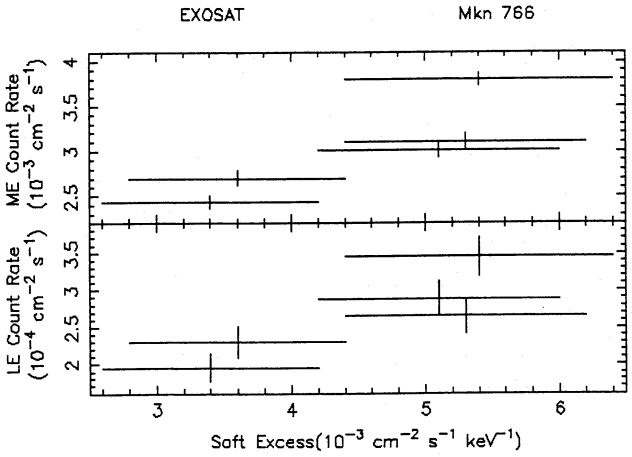

Figure 8. Plots of the LE and ME count rates versus soft excesses of Mkn 766 which show the correlated variabilities.

width, but lack of low-energy absorption, could be explained by a warm absorber or partial-covering models (Yaqoob, Warwick & Pounds 1989; Pounds et al. 1989). Runs made with a partial-covering model, however, show that there were no improvements in the χ^2_r values over those obtained from the power-law plus fixed-absorption plus Gaussian-line model. The results of the present paper therefore suggest that the fluorescence from warm material can produce a high fluorescence yield for the iron line, but negligible low-energy absorption.

ACKNOWLEDGMENTS

We are grateful to Professor J. C. Bhattacharyya for his support and encouragement, and to the *EXOSAT Observatory* staff, especially Drs N. E. White, A. N. Parmer, F. Habrel, P. Giommi, P. Barr and A. M. T. Pollock at ESTEC who helped us to get the data from the archives and provided us with the XSPEC software package. One of us, KKG, thanks the *EXOSAT* staff for their help in data analysis. Our sincere thanks are due also to the referee for valuable comments.

REFERENCES

Arakelian M. A., Dibai E. A., Esipov V. F., Markarian B. E., 1971, Astrophys., 7, 102
Bell Burnell S. J., Chiappetti L., 1984, A&AS, 56, 415
Cooke B. A. et al., 1978, ApJ, 222, L91
de Bruyn A. G., Wilson A. S., 1976, A&A, 53, 93
de Korte P. A. J., Bleeker J. A. M., den Boggende A. J. F., Branduardi-Raymont G., Culhane J. L., Gronenschild E. H. B. M., Mason I., McKechnie S. P., 1981, Space Sci. Rev., 30, 495
De Grijp M. H. K., Miley G. K., Lub J., de Jong T., 1985, Nat, 314, 240
Denisyuk E. K., Lipovetski V. A., 1974, Astrophys., 10, 195
Denisyuk, E. K., Lipovetski, V. A., 1977, Soviet Astron. J. Lett., 3, 3
Dower R. G., Griffiths R. E., Bradt H. V., Doxsey R. E., Johnston M. D., 1980, ApJ, 235, 355
Elvis M., Lockman F. J., Wilkes B., 1989, AJ, 97, 777
Elvis M., Maccacaro T., Wilson A. S., Ward M. J., Penston M. V., Fosbury R. A. E., Perola G. C., 1978, MNRAS, 183, 129
Fairall A. P., 1977, MNRAS, 180, 391
Ghosh K. K., Soundararajaperumal S., 1991a, AJ, 102, 1298

Ghosh K. K., Soundararajaperumal S., 1991b, ApJ, 383, 574
Ghosh K. K., Soundararajaperumal S., 1992, ApJ, 389, 179
Ghosh K. K., Soundararajaperumal S., Kalaiselvi M., Sivarani T., 1991, A&A, 255, 119
Giacconi R. et al., 1974, ApJS, 27, 34
Glass I. S., 1985, Mon. Not. Astron. Soc. S. Afr., 44, 60
Hayakawa S., 1991, Nat, 351, 214
Hayes M. J. C., Culhane J. L., Bell Burnell S. J., 1980, MNRAS, 192, 1P
Heiles C., 1975, A&AS, 20, 37
Kriss G. A., Canizares C. R., Ricker G. R., 1980, ApJ, 242, 492
Kriss G., Doxsey R., 1983, PASP, 95, 133
Krolik J. H., Kallmann T. R., 1987, ApJ, 320, L5
Kruper J. S., Urry C. M., Canizares C. R., 1990, ApJS, 74, 347
Kunieda H., Turner T. J., Awaui H., Koyama K., Mushotzky R., Tsusaka Y., 1990, Nat, 345, 789
Lampton M., Margon B., Bowyer S., 1976, ApJ, 208, 177
Leighly K. M., Pounds K. A., Turner T. J., 1989, in Hunt J., Battrick B., eds, Proc. 23rd ESLAB Symp. on Two Topics in X-ray Astronomy. ESA SP-296, ESA, Noordwijk, p. 961
Lonsdale C. J., Helou G., Good J. C., Rice W., 1985, Cataloged Galaxies and Quasars Observed in the IRAS Survey. Jet Propulsion Laboratory, Pasadena
McHardy I. M., Lawrence A., Pye J. P., Pounds K. A., 1981, MNRAS, 197, 893
Markarian B. E., 1969, Astrophys., 5, 286
Markarian B. E., Lipovetski V. A., 1971, Astrophys., 7, 299
Markarian B. E., Lipovetski V. A., 1972, Astrophys., 8, 89
Markarian B. E., Lipovetski V. A., 1976, Astrophys., 12, 241
Marshall F. E., Boldt E. A., Holt S. S., Mushotzky R. F., Pravdo S. H., Rothschild R. E., Serlemitsos P. J., 1979, ApJS, 40, 657
Morrison R. & McCammon D., 1983, ApJ, 270, 119
Mushotzky R. F., 1984, Adv. Space Res., 3, 157
Osterbrock D. E., 1977, ApJ, 215, 733
Osterbrock D. E., De Robertis M. M., 1985, PASP, 97, 1129
Pounds K. A., Nandra K., Stewart G. C., Leighly K., 1989, MNRAS, 240, 769
Pounds K. A., 1989, in Hunt J., Battrick B., eds, Proc. 23rd ESLAB Symp. on Two Topics in X-ray Astronomy. ESA SP-296, ESA, Noordwijk, p. 753
Pounds K. A., Nandra K., Stewart G. C., George I. M., Fabian A. C., 1990, Nat, 344, 132
Reichert G. A., Wu C.-C., Boggess A., Oke J. B., 1985, BAAS, 17, 578
Simkin S. M., Su H. J., Schwarz M. P., 1980, ApJ, 237, 404
Stark J. P., Bell Burnell S. J., Culhane J. L., 1978, MNRAS, 182, 23P
Tananbaum H., Peters G., Forman W., Giacconi R., Jones C., Avni Y., 1978, ApJ, 223, 74
Tennant A. F., Mushotzky R. F., 1983, ApJ, 264, 92
Turner M. J. L. T., Smith A., Zimmermann H. U., 1981, Space Sci. Rev., 30, 513
Turner T. J. et al., 1989, in Hunt J., Battrick B., eds, Proc. 23rd ESLAB Symp. on Two Topics in X-ray Astronomy. ESA SP-296, ESA, Noordwijk, p. 769
Turner T. J., Pounds K. A., 1989, MNRAS, 240, 833
Ulvestad J. S., Wilson A. S., 1984, ApJ, 285, 439
Urry C. M. et al., 1987, in Treves A., ed., Variability of Galactic and Extragalactic X-ray Sources. Associazione per l'Avanzamento dell' Astronomica, p. 15
Urry C. M., Arnaud K., Edelson R. A., Kruper J. S., Mushotzky R. F., 1989, in Hunt J., Battrick B., eds, Proc. 23rd ESLAB Symp. on Two Topics in X-ray Astronomy. ESA SP-296, ESA, Noordwijk, p. 789
Walker M. F., Chincarini G., 1967, ApJ, 147, 416
Weedman D. W., 1973, ApJ, 183, 29
West R. M., Danks A. C., Alcaino G., 1978, A&A, 65, 151
West R. M., 1979, IAU Circ., 3415
West R. M., Grosbol P., Sterken C., 1980, ESO preprint N101
Wilkes B. J., Elvis M., 1987, ApJ, 323, 243
Wilkes B. J., Masnou J.-L., Elvis M., McDowell J., Arnaud K., 1989, in Hunt J., Battrick B., eds, Proc. 23rd ESLAB Symp. on Two Topics in X-ray Astronomy. ESA SP-296, ESA, Noordwijk, p. 1081
Wood K. S. et al., 1984, ApJS, 56, 507
Yaqoob T., Warwick R. S., Pounds K. A., 1989, MNRAS, 236, 153